STScI | SPACE TELESCOPE SCIENCE INSTITUTE

Instrument Science Report STIS 2017-05(v1)

STIS CCD Performance through Cycle 24

Allyssa Riley[1], John Debes[1], Sean Lockwood[1]

[1] Space Telescope Science Institute, Baltimore, MD

29 September 2017

ABSTRACT

This report summarizes the overall performance of the STIS CCD since Servicing Mission 4 (SM4). Overall, the dark current and hot pixels have remained stable. The gain values using all three available amplifiers were remeasured and they have also continued to be stable. The read noise for amplifiers C and D have both exhibited substantial increases within the last few years. The charge transfer efficiency (CTE) was indirectly measured using the Extended Pixel Edge Response (EPER) Test, which shows both the parallel and serial CTE has continued degrading over time.

Contents

Operated by the Association of Universities for Research in Astronomy, Inc., for the National Aeronautics and Space Administration.

1. Introduction

The Space Telescope Imaging Spectrograph (STIS) has been on-board the Hubble Space Telescope (HST) for over 20 years. In 2001, four years after STIS was installed, the first side of electronics failed and STIS was switched over to its redundant side-2 electronics. In 2004, side-2 also failed and it was not until 2009, during Servicing Mission 4 (SM4), that the side-2 electronics were restored. Although side-2 is the redundant side, it differs from side-1 in that it does not contain a working temperature control unit to measure and regulate the temperature of the CCD itself. Instead, the STIS Team uses the CCD housing temperature as a proxy for the detector temperature, but this lack of direct detector temperature control proves difficult to account for in some of the monitors presented in this report.

Throughout the last two decades, the STIS team has monitored the health and stability of the CCD, including measuring the gain, read noise, dark current, hot pixels, charge transfer efficiency (CTE), and extended pixel edge response (EPER).

Each cycle, the STIS team invests 1355 parallel internal orbits to calibration programs, over 1200 of which monitor the CCD, to provide better science to the astronomical community. All of the programs discussed in this document are regular programs that are run every cycle. The last documentation of the overall performance of the CCD was in 2009 (Goudfrooij, et al 2009) but in cycles 18-21, the STIS team prepared cycle close-out reports that detailed the results of each of the monitors.

In each section of this document, we give background on the relevant monitoring programs and report the results of each program up through the middle of Cycle 24.

2. CCD Gain Values

Because the gain of a detector is a proxy for detector health, the STIS team monitors the CCD gain every cycle with the STIS CCD General Performance Monitor (e.g., Cycle 24 PID: 14816, PI: Riley). This program takes bias and flat field observations every six months, in March and September. For each mode, two biases and two flat frames are taken. The gain calculated using these observations is given by:

$$g = \frac{\text{mean}(flat_1) + \text{mean}(flat_2) - \text{mean}(bias_1) - \text{mean}(bias_2)}{\sigma^2_{diff\_flat} - \sigma^2_{diff\_bias}} \quad (1)$$

where $flat_1$ and $flat_2$ are the two flat frames, $bias_1$ and $bias_2$ are the two bias frames and $diff\_bias$ and $diff\_flat$ are the differences between the two biases and the two flats, respectively (Goudfrooij, et al 2009).

Because amplifier D has the lowest read noise and is therefore the most commonly-used and only supported amplifier, the General Performance Monitor only calculates the gain with amplifier D.

The STIS team does not regularly monitor the other amplifiers, so a special calibration program was proposed and accepted for Cycle 23 (PID: 14424, PI: Biretta). The

goal of this program was to determine the STIS CCD gain for amplifiers A, C, and D and with gain settings of 1 and 4 e^-/DN using the mean-variance method. This method involves plotting the variance of a difference flat frame as a function of the mean of an average flat frame at different exposure times, and thus different flux levels. The gain is given by the inverse of the slope of this line.

More information about both methods described above can be found in the STIS ISR 2016-01 (Riley, et al. 2016).

2.1 Analysis and Results

The gain values calculated using the observations from the General Performance Monitor have remained steady since operations to STIS were resumed in 2009 (see Figure 1).

In Figure 1, we see that the results for the General Performance Monitor agree well with the results calculated with the mean-variance technique. This means that, despite the fact that the method used for the General Performance Monitor is a less exact method than the mean-variance method, it produces results close enough to the value that the STIS team has adopted for the CCD reference files, 1.0 and 4.016 e^-/DN (Goudfrooij, et al. 2009). This similarity in the results tells us that we do not need to change the way we monitor the CCD gain value. The method used now requires little telescope time and very few resources to calculate, unlike the mean-variance method.

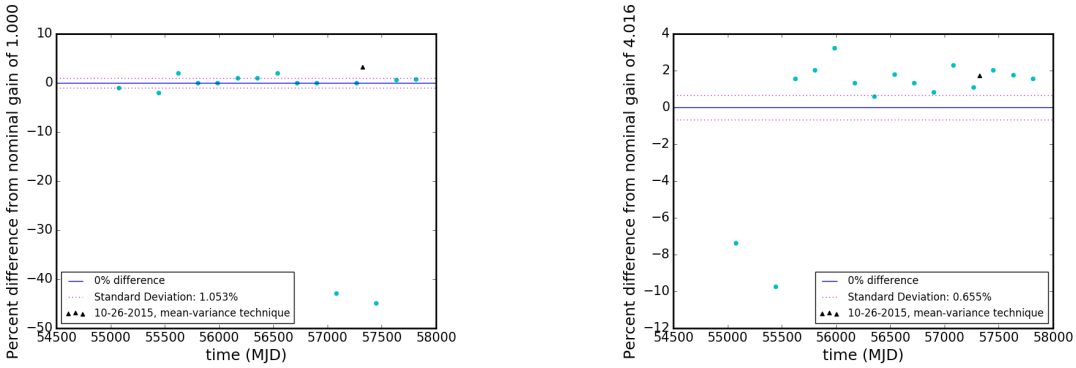

(a) GAIN = 1

(b) GAIN = 4

Figure 1.: The percent discrepancies in amplifier D compared to gains 1.000 and 4.016 e^-/DN, using the results of the STIS General Performance Monitors from March 2009 through March 2017. The solid blue lines indicate where the results agree with the nominal gain values that are used in the STIS pipeline. The dotted magenta lines indicate where one standard deviation of the data lies. Finally, the black triangles indicate where on the plot the gain calculated with the mean-variance technique for the special calibration program 14424 lie.

The mean-variance method of calculating the gain indicates a $< 3.5\%$ change in the gain since previously measured using the same technique, pre-flight. The General Performance Monitor shows constant gain (Figure 1) and the discrepancy between the General Performance Monitor results and those from the mean-variance method are due to differences in the two methods.

It should be noted that, in Figure 1a, there are two discrepant points where the gain was calculated to be 0.7 and 0.69 e^-/DN. We found that the method used in the General Performance Monitor is susceptible to cosmic rays and this caused the low data points. Thus, we decided to reject them from our standard deviation calculation. Figure 1b has similar low data points, which have also been rejected from our analysis.

More detailed description of the mean-variance method, the full analysis, results and conclusion of this program can also be found in the STIS ISR 2016-01 but the results are summarized in Table 1 below.

Amplifier	Nominal Gain (e^-/DN)	Measured Gain (e^-/DN)	Percent Discrepancy
A	1	1.028 ± 0.001	2.80
A	4	3.993 ± 0.007	0.18
C	1	0.991 ± 0.001	0.90
C	4	4.100 ± 0.007	2.50
D	1	1.034 ± 0.003	3.40
D	4	4.087 ± 0.007	1.77

Table 1.: The measured gain values, according to the mean-variance technique per mode, as well as the percent discrepancies between the measured and nominal gains. Taken from Riley, et al. 2016.

2.2 Software Updates

Although we found that the results from the method used in the General Performance Monitor agree well with the gain values adopted in the STIS CCD reference files (see Figure 1), there were still some changes that needed to be made to the General Performance Monitor. We found that the gain calculation script contained bugs and was not as rigorous as it should have been. To calculate a more accurate gain value, we rewrote the gain calculation script so that it sorts the observations by mode (aperture, filter, binning, etc.), outputs the gain values for each mode, and uses all of the available data taken as part of the General Performance Monitor program.

This new script as well as the script used to calculate the gain via the mean-variance technique are available for use in the future. Both of these new scripts are available on grit.stsci.edu.

3. CCD Read Noise

The read noise of the STIS CCD is calculated using the observations from the STIS CCD Bias and Read Noise Monitoring Program (Cycle 24 PIDs: 14820 and 14821). Each day, 14 bias frames were taken with a gain setting of 1 e^-/DN and 3 were taken with a gain setting of $4e^-/DN$. The biases between anneals were used to create the bias reference files for that anneal period for both gain settings 1 and 4 e^-/DN.

The read noise is calculated using the following equation:

$$RN = gain * \frac{\sigma_{bias_1 - bias_2}}{\sqrt{2}} \tag{2}$$

where $\sigma_{bias_1 - bias_2}$ is the standard deviation of the difference bias.

The CCD General Performance Monitor also calculates the read noise independent of the Read Noise Monitor. It uses equation 2 with the biases taken as part of the

General Performance Monitor Program.

3.1 Analysis and Results

The primary amplifier used in science observations is amplifier D and a plot of the read noise over time is shown in Figure 2. There was a substantial jump in the read noise for amplifier D at gain setting 1 e^-/DN in mid-2014, due to a cosmic ray's interaction with the amplifier D electronics. Despite this jump, amplifier D is still the main amplifier used in science observations because it has the lowest read noise of any of the amplifiers on STIS.

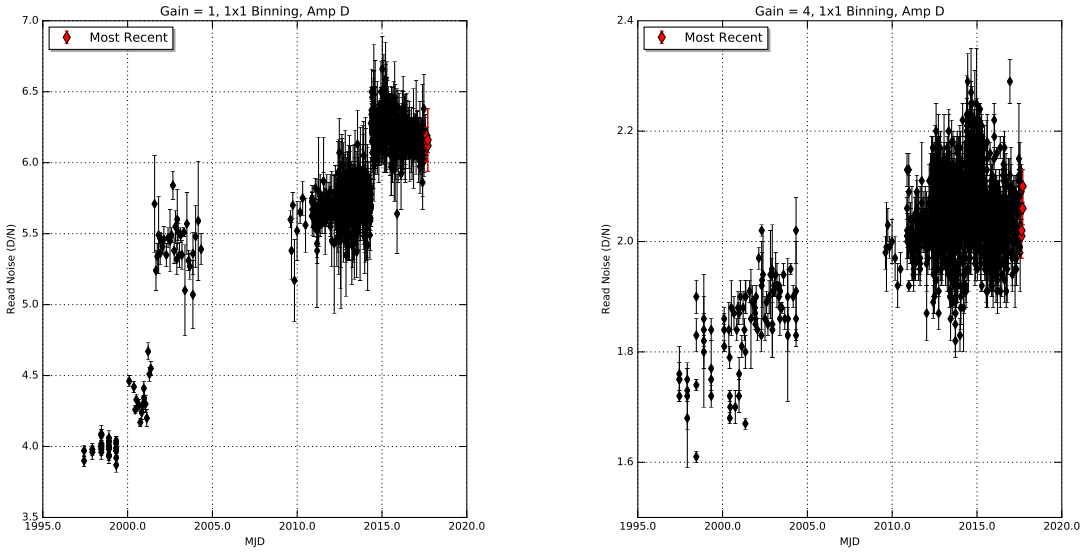

(a) GAIN = 1

(b) GAIN = 4

Figure 2.: The read noise of amplifier D over time. The red diamonds represent the six most recent measurements, taken 15 through 18 August and 11 through 12 September 2017.

On 11 Sept. 2016, amplifier C experienced a similar jump in read noise (see Figure 3). The jump in the GAIN = 1 setting is much more obvious than the one seen in the GAIN = 4 setting because of the amount of scatter and variability in the read noise values for the GAIN = 4 setting. The GAIN = 1 and GAIN = 4 settings exhibit percent changes of $\sim$7% and $\sim$4.5%, respectively.

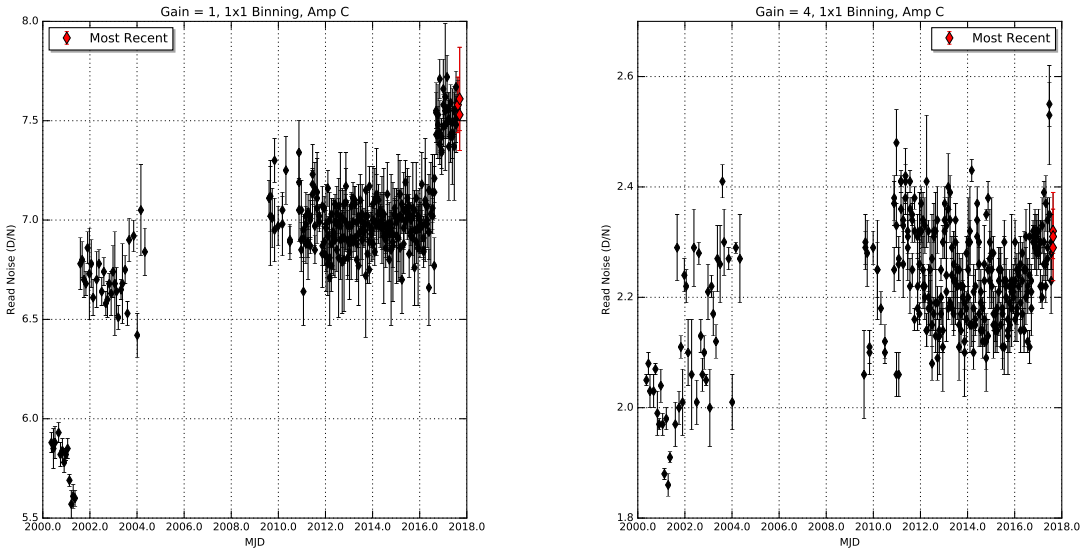

(a) GAIN = 1

(b) GAIN = 4

Figure 3.: The read noise of amplifier C over time. The red diamonds represent the three most recent measurements, taken 15 August and 11 through 12 September 2017.

The STIS team also monitors the read noise in Amplifier A. As seen in figure 4, the read noise for amplifier A has been steadily increasing over time but has not experienced any large, sudden changes, such as those in amplifiers C and D.

Although amplifiers A and C are not used in science exposures or to create CCD reference files, they are still useful in helping to determine the charge transfer efficiency (CTE) of the STIS CCD. In particular, the CCD Sparse Field CTE Monitoring Program (Cycle 24 PID: 14826, PI: Lockwood) utilizes amplifiers A and C at gains 1 and 4 to calculate the parallel CTE. For more detailed information about the sparse field program, refer to STIS ISR 2006-01. The results from these programs are used to update the STIS CCDTAB if needed. For more information about the CTE, see Section 5.

Amplifiers A and C are also used to measure the detector sensitivity using the Full Field Sensitivity survey, which takes images of the Omega Cen star field. The photometry of these stars compared to the expected value reveals the sensitivity of the CCD across the full field of view. For more information, see STIS ISR 2013-02 (Roman-Duval & Proffitt, 2013).

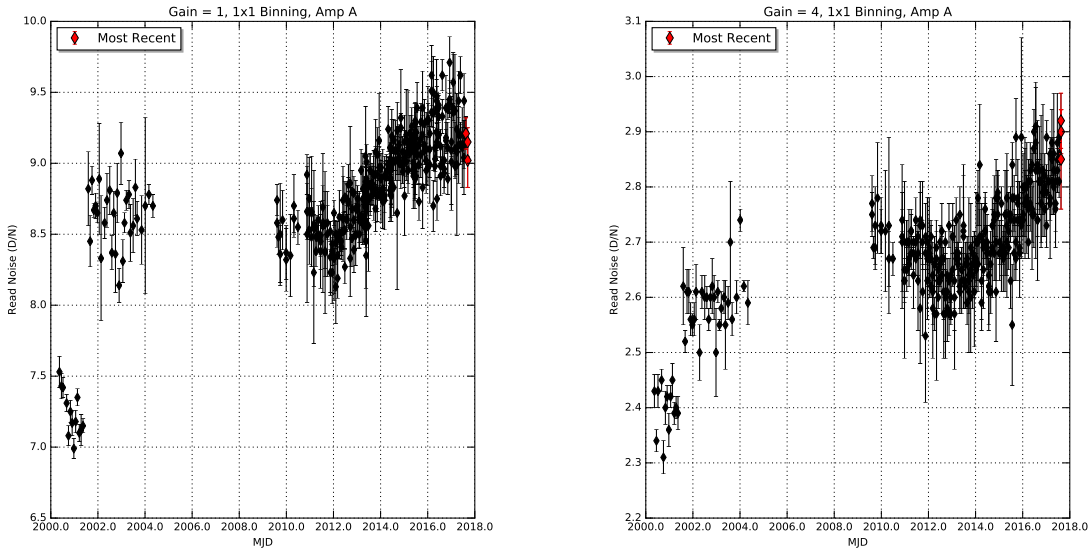

(a) GAIN = 1

(b) GAIN = 4

Figure 4.: The read noise of amplifier A over time. The red diamonds represent the three most recent measurements, taken 15 August and 11 through 12 September 2017.

In Cycle 23, the STIS team recalculated the read noise values that are used in the CalSTIS pipeline to calibrate the science data. We found that, in the past, the read noise for CalSTIS had been calculated for each time period using the mean of only the preliminary read noise measurements. This time, we used the entirety of the measurements for a given period in order to find the most accurate value. For more detailed information about this update and its effects, please see STIS STAN August 2016 (STIS Team, 2016).

4. Hot Pixel Annealing and Dark Current

Due to the accumulation of radiation on the CCD, the dark current is expected to increase over time. This photon radiation causes damage to the CCD pixels, causing hot and warm pixels. These pixels can return to their lower dark current by annealing the CCD.

The STIS CCD Hot Pixel Annealing program (Cycle 24 PID: 14822, PI: Riley) includes warming the CCD from ~ -83°C to ~ 5°C for 12 hours and then cooling it back down, repeating this procedure monthly. The hot pixel annealing program is meant to track the creation of hot pixels over time and to investigate how the annealing process affects the dark current. This program takes dark, bias, and flat frames both before and after the anneal.

4.1 Hot Pixel Annealing

Figure 5 shows the increasing number of hot pixels despite the monthly anneals. We suspect that the scatter in the post-SM4 data is due to some fundamental differences in how the STIS team calculates the hot pixels now when compared to pre-SM4. Unfortunately, because we do not have access to the old anneal monitoring scripts, we cannot confirm this suspicion.

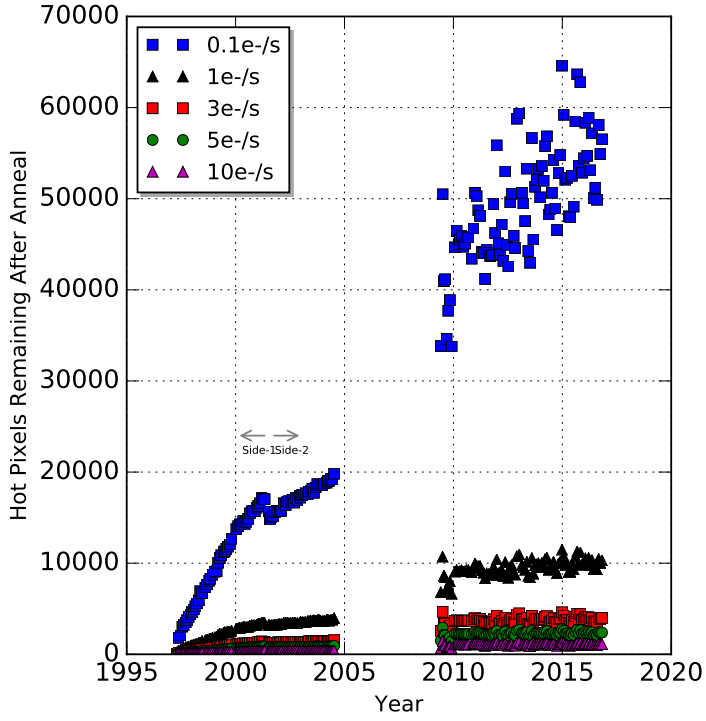

Figure 5.: The number of hot pixels remaining after each anneal using 5 different cut-offs.

The STIS team currently uses a temperature correction that corresponds to 7% increase in dark rate per degree and is scaled to 18°C (Brown, 2001). Recently, we have seen that the anneals appear to be ineffective at decreasing the number of hot pixels. Over the last 12 anneals, five of them have shown an increase in hot pixels after the anneal. We suspect this could be because the number of pixels that are consistently hot (that is, hot in every observation) has increased.

This scatter could indicate that the temperature correction that we have been using is incorrect. The last time the temperature correction was calculated was in 2001 (see STIS ISR 2001-03) and was revisited in 2012 with results published in STIS ISR 2012-

02. In this 2012 ISR, the author notes that, despite finding a different temperature correction than Brown did in 2001 (9%/degree vs. 7%/degree), the errors were large and encompassed Brown's results. For this reason, the author decided not to revise the temperature correction (Mason, 2012). The STIS Team is currently in the process of revisiting the temperature dependence of the dark rate again and we expect there to be a time dependence as well as a temperature dependence.

In the meantime, we studied two consecutive anneal periods, to determine whether the anneals are, in fact repairing any pixels. Just plotting the number of pixels in each dark frame across an anneal period shows a large scatter of a few thousand pixels and would lead one to believe that the anneals are ineffective. However, we found that the number of consistently hot pixels, those that are not repaired by anneals, overwhelms the number of non-consistently hot pixels. In Figure 6, the number of pixels greater than $0.1e^{-}/s$ is plotted across 2 anneal periods. This plot does not include hot pixels from the previous superdark, which was used as a proxy for consistently-hot pixels. We masked the pixels in the previous superdark that were greater than $0.1e^{-}/s$ and used that to filter out the pixels in the darks across two anneals that corresponded to the consistently-hot pixels. Then, we temperature corrected the darks, median combined them in groups of five, and found where the dark rate is greater than $0.1e^{-}/s$. Figure 6 shows something similar to what we would expect; the number of hot pixels increases over an anneal period and decreases during the anneal.

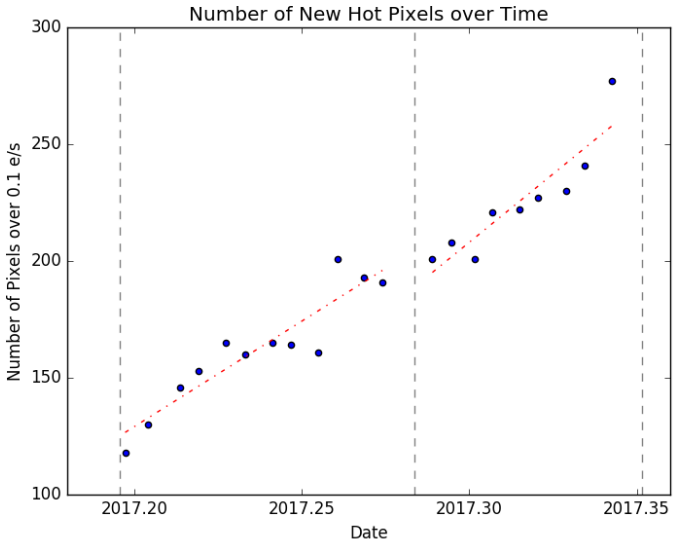

Figure 6.: The number of hot pixels in dark frames taken between anneals, not including consistently-hot pixels.

This study showed us that the anneal monitor, as it is now, is not robust enough

to accurately monitor the repairing of hot pixels. It does not filter out the consistently hot pixels and it combines three darks as opposed to five, like above, so it is affected more significantly by cosmic rays. These reasons explain why we don't see the anneals consistently working to repair pixels (see the anneal statistics on the anneal monitoring webpage). The next step for the STIS team is to implement a version of this more robust analysis in the anneal monitor.

The results of the anneal monitor are published monthly on the STIS Anneal webpage.

4.2 Dark Current

The dark current is measured monthly by using the dark frames taken with the CCD Hot Pixel Annealing program, by finding the mean of the dark frame after the anneal. Figure 7 shows how the median dark rate has changed over the lifetime of STIS. Like the hot pixels shown in Figure 5, there is a substantial increase in the scatter after SM4 in 2009. We suspect it is due to the detector CTE and the fact that the total noise in each pixel does not follow the theoretical behavior (Mason, 2012). We would expect the noise to consist of the dark rate Poisson noise and the read noise, however the data is showing a higher scatter than would be expected given the theoretical model. It is possible that this scatter is due to detector CTE. Systematic problems with the temperature correction could also be contributing to the scatter.

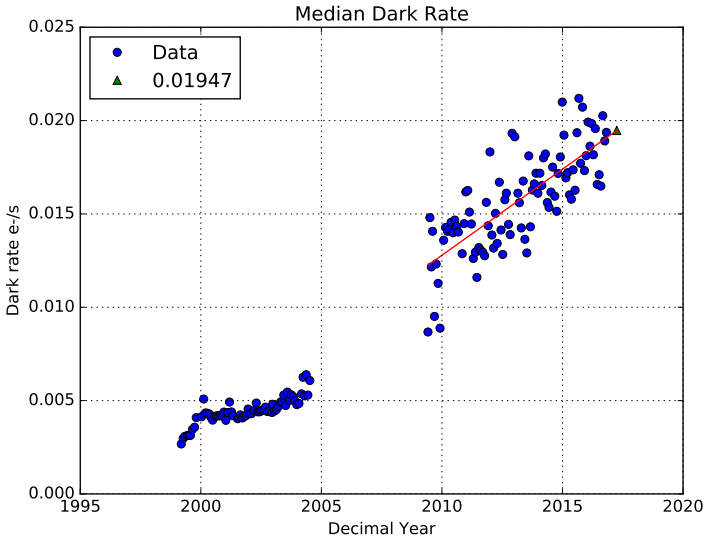

Figure 7.: The dark rate is measured after each anneal. The blue points denote the measured dark current, the red line marks the fitted line according to the measurements and the green triangle shows the projection of the dark rate in mid-Cycle 25.

The most recent measurement of the STIS CCD dark rate was at 0.01937 e-/s, the median calculated dark rate was 0.0184 e-/s for Cycle 23, and the dark rate currently used for calibrating the STIS data is 0.018 e-/s.

The STIS CCD Dark Rate Monitoring Program has been run each cycle to track the dark rate. The 1100 second dark frames taken twice each day are used to produce the dark reference files that are used to calibrate science data. Four 60 second dark frames are taken daily as well. All observations are taken using amplifier D and at a gain setting of 1 e^-/DN.

Beginning in Cycle 20 up through Cycle 23, in addition to the routine dark frames using amplifier D, we replaced two daily 60 second dark frame visits using amplifier D with 60 second darks using amplifier A for 30 days to better characterize the CTE. This will be discussed further in Section 5

Recently, it was found that superdark reference files between June 2 and December 9, 2009 as well as June 23 through August 4, 1998 were corrupted. More specifically, they were created with not only 1100 second darks, but also 60 second darks, increasing the noise level in the superdarks. Figure 8 shows a comparison of a supernova spectrum taken in the later half of 2009 using the corrupted darks (bottom panel) versus the newly reprocessed darks (top panel).

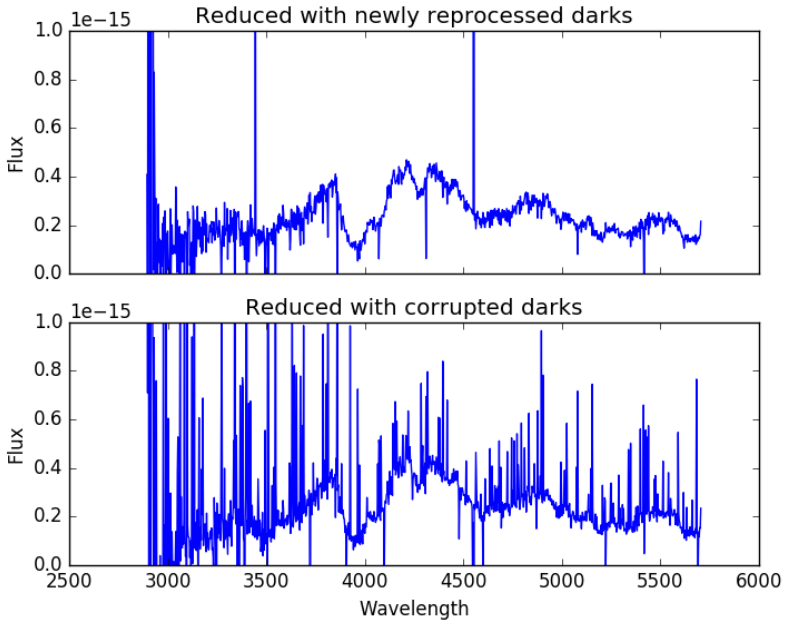

Figure 8.: The top panel shows the supernova spectrum (obd702010) with the newly reprocessed darks and the bottom panel shows the spectrum with the old, corrupted darks.

In STIS ISR 2011-02(v2), this noise seen in the spectrum of the bottom panel of Figure 8 was attributed to poor CTE (Van Dyke Dixon, 2011). Figure 8 shows that, although CTE could be contributing to the noise level, it is predominantly caused by the corrupted darks.

These bad darks from 2009 have been updated using only 1100 second darks.

4.3 Analysis and Results

All 1100 second dark frames taken between anneals are combined to produce a superdark reference file. The baseline bias level is corrected for using the superbias file created for the same anneal period.

The average median dark rate calculated in recent anneal periods is ~ 0.0192e/s. This is what we would expect, given the dark rate projection for mid-Cycle 25

5. CCD Charge Transfer Efficiency

Exposure to high radiation can cause pixel traps in the CCD, which cause a decrease in the CTE or an increase in the Charge Transfer Inefficiency (CTI). CTE is the ability of

the detector to transfer the charge of a pixel between adjacent pixels (Goudfrooij, et al 2006) and CTI is 1-CTE. CTE loss causes the flux of sources to appear lower than if the detector had no pixel traps. An example of CTE can be seen in figure 9.

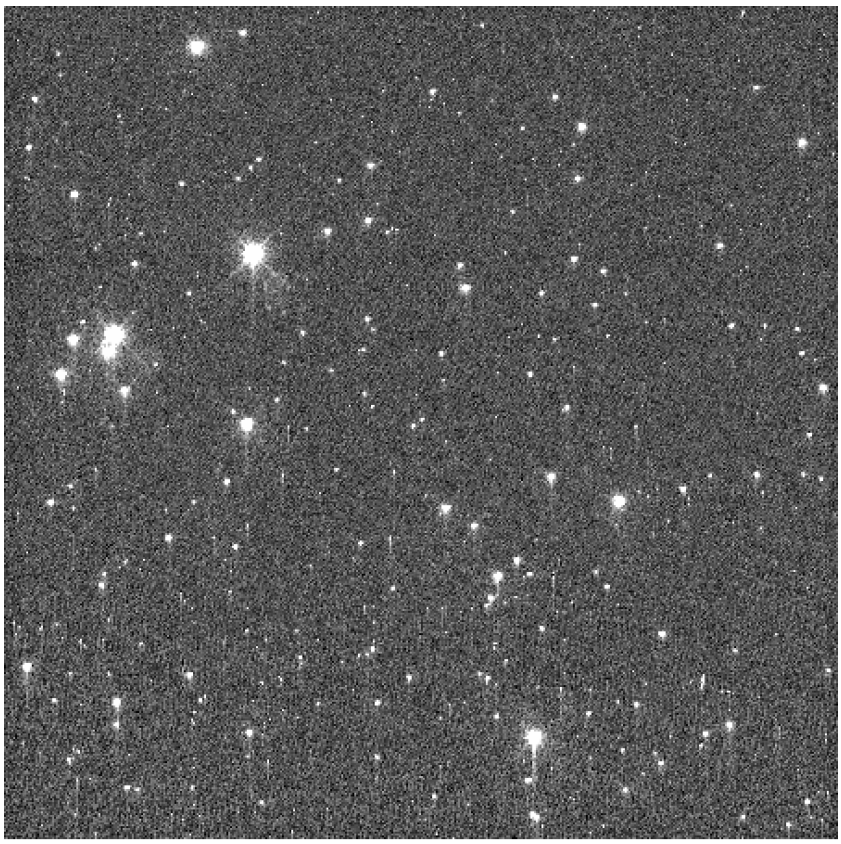

Figure 9.: The CTE loss can be seen in this image (obmj01050) as the flux trails underneath the sources. For STIS, the most significant CTE loss is in the Y direction, called parallel CTE (Van Dyke Dixon, 2011). The amplifier is located at the top of the detector and the trails are caused by a delay in the release of charge during readout.

The General Performance Monitor uses the Extended Pixel Edge Response (EPER) test to make an indirect calculation of the CTE (Janesick, et al. 1991). The EPER test uses the overscan region of the detector to measure the charge after it's been bias corrected (Goudfrooij, et al. 2009). It is important to note that the EPER test does not measure the absolute CTE but provides a good measure of the relative CTE (Goudfrooij, et al., 2009). More information about the EPER test is available in STIS ISR 2009-02. This test is run every six months and the results are shown in figure 10.

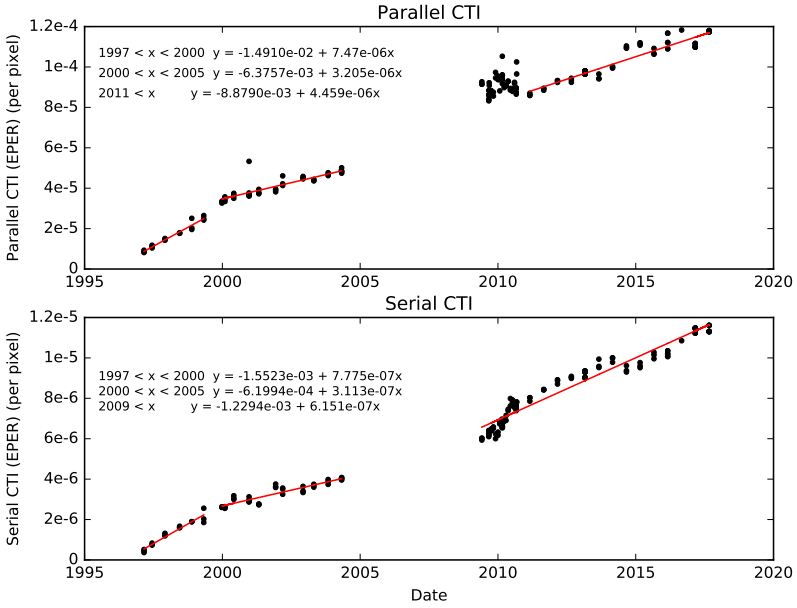

Figure 10.: CTE loss in the STIS CCD is most significant in the parallel direction. The CTI in the parallel direction is an order of magnitude larger than in the serial direction. Both the parallel and serial CTI has continued to increase at roughly the same rate as pre-SM4.

The STIS Team also uses the Sparse Field program (Cycle 24 PID: 14826, PI: Lockwood) to measure the CTE. The Sparse Field program projects a narrow slit using the on-board lamp onto five different positions on the detector (Goudfrooij, et al. 2006). Various exposures are taken at each position, alternating the read-out amplifier used between A and C. The further the charge in the pixels has to travel to be read out, the more charge will be lost.

STIS ISR 2006-01 provides in-depth detail about this program, as well as results between 1999 and 2004. More recent data is currently being analyzed but figure 11 shows the preliminary results.

Figure 11 was created using data from the Sparse Field program (discussed in Section 3). This program takes data at various locations along the y-axis of the CCD and reads the data out at either the top or bottom of the detector. This information gives us the empirical value of the CTE for the STIS CCD. These values are used to update the empirical CTE coefficients in the CCDTAB, which tells the calibration pipeline the amount of CTI data at a specific place on the CCD experiences. Figure 11 shows that, as time goes on, the CTI increases at lower flux values but then converges to zero at the highest fluxes.

It is important to note that, because this analysis is ongoing, the absolute measurements of CTI in figures 11 is still to be determined but the relative CTI is correct.

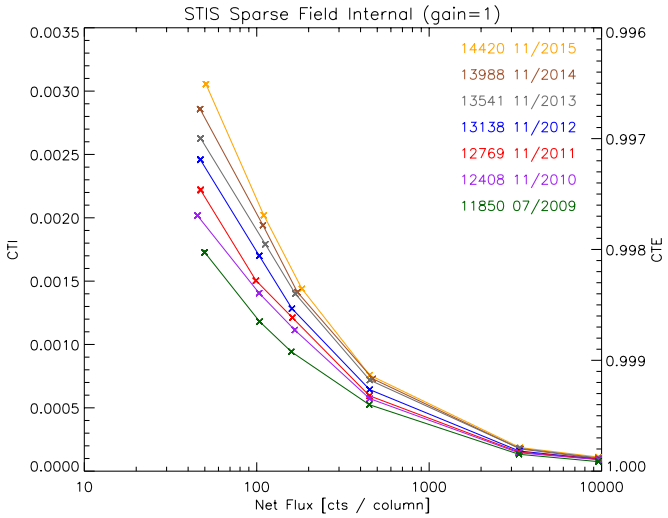

Figure 11.: Over time, the CTI has increased at the lowest flux levels but ends up converging to 0 at the highest flux levels. Note that the absolute CTI is still to be determined, but the relative CTI is correct.

Acknowledgements

We thank the STIS team for insightful discussions about the performance of the CCD and for taking the time to edit this document.

Change History for STIS ISR 2017-05

Version 1: 29 September 2017- Original Document

References

Brown, T. 2001, "Temperature Dependence of the STIS CCD Dark Rate During Side-2 Operations." STIS ISR 2001-03

Goudfrooij, P., Maiz-Apellaniz, J., Brown, T., Kimble, R. 2006, "Charge Transfer Efficiency of the STIS CCD: The Time Dependence of Charge Loss and Centroid Shifts from Internal Sparse Field Data." STIS ISR 2006-01

Goudfrooij, P., Wolfe, M.A., Bohlin, R.C., Proffitt, C.R., Lennon, D.J. 2009, "STIS CCD Performance After SM4: Read Noise, Dark Current, Hot Pixel Annealing, CTE,

Gain, and Spectroscopic Sensitivity." STIS ISR 2009-02
Janesick, J. R., Soli, G., Elliot, T., & Collins, S., 1991, The effects of proton damage on charge-coupled devices, in Proc. SPIE, 1447, 87.
Mason, E. 2012, "Post SM4 Behavior of the STIS CCD Darks." STIS ISR 2012-02
Riley, A., Monroe, T., Lockwood, S. 2016, "Determination of the STIS CCD Gain." STIS ISR 2016-01
Roman-Duval, J. & Proffitt, C. 2013, "Full-field sensitivity and its time-dependence for the STIS CCD and MAMAs." STIS ISR 2013-02(v1)
STIS Team. 2016, "Updated Read Noise Values for the STIS/CCD in the CCDTAB Released." STIS STAN August 2016
Van Dyke Dixon, W. 2011, "Effects of CTE Degradation on Cycle 18 Observations with the STIS CCD." STIS ISR 2011-02(v2)